Considering Streamflow Trend Analyses Uncertainty in Urbanizing Watersheds: A Baseflow Case Study in the Central United States

Jason A. Hubbart*

Department of Forestry, and Department of Soils, Environmental and Atmospheric Sciences, University of Missouri, Columbia, Missouri

Chris Zell

Interdisciplinary Hydrology Laboratory, University of Missouri, Columbia, Missouri

Received 11 September 2012; accepted 31 March 2013

ABSTRACT: Assuming pro rata reductions in baseflow resulting from urban development may not be valid in all urbanizing watersheds. Anthropogenic offsets or compensatory contributions to baseflow (e.g., net exfiltration from sewer lines, wastewater effluents, and lawn irrigation) may mask or confound fundamental changes in hydrologic pathways. These offsets illustrate the complexities of urban flow processes and the need for improved understanding to mitigate urban development impacts. The authors used two dissimilar automated baseflow separation algorithms and Monte Carlo techniques to evaluate urban baseflow and estimation uncertainty using data from a representative urban watershed in the central United States. Three uncertainties affecting trend determinations were assessed, including algorithm structure, precipitation–runoff relationships, and baseflow algorithm parameterization. Results indicate

* Corresponding author address: Dr. Jason A. Hubbart, Department of Forestry and Department of Soils, Environmental and Atmospheric Sciences, University of Missouri, 203-Q ABNR Building, Columbia, MO 65211.

E-mail address: hubbartj@missouri.edu

DOI: 10.1175/2012EI000481.1

that, despite ongoing population growth and development, annual streamflow metrics in the authors' representative watershed have not significantly increased or decreased ($p > 0.05$) from 1967 to 2010. However, several streamflow metrics featured shallow insignificant ($p > 0.05$) slopes in the direction hypothesized for an urbanizing (less pervious) watershed, including a downward slope for baseflow index (BFI) and increases in runoff volume coefficient. Median annual baseflow estimations differed by 29% between techniques (85.3 versus 118.9 mm yr^{-1}). In the absence of direct tracer measurements, uncertainties associated with precipitation–runoff relationships, algorithm structure, and parameterization should be included in analyses evaluating alterations from baseline hydrologic conditions in urban watersheds. To advance application of separation algorithms for urban watersheds and support regulatory reductions in runoff volume, future work should include calibration of model parameters to available hydrogeologic and tracer data.

KEYWORDS: Urban watersheds; Hydrology; Baseflow; Modeling uncertainty

1. Introduction

Urban waterways and resident aquatic communities are exposed to several anthropogenic stressors or risks that may occur less frequently or be entirely absent in watersheds that have predominantly rural but mixed land uses (Walsh et al. 2005; Wenger et al. 2009). Hydrogeomorphic impacts stemming from reapportionment of freshwater supplies in urbanizing environments include (but are not limited to) channel incision, streambed sedimentation, increased contaminant transport, altered hydrologic connectivity, and habitat degradation (Paul and Meyer 2001; Lerner 2002; Sophocleus 2002). Aquatic habitat and biota in natural systems are sustained between runoff events by groundwater contributions to streamflow, termed "baseflow" (Sophocleus 2002). Reductions in recharge caused by impervious surfaces were hypothesized as rationale for declining baseflows in selected urban environments (Bernhardt and Palmer 2007; O'Driscoll et al. 2010). However, as Lerner (Lerner 2002) and Meyer (Meyer 2005) explicate, the assumption of pro rata reductions in baseflow resulting from increased impervious surfaces may not be valid in all urbanizing watersheds. Rather, anthropogenic offsets or compensatory contributions to baseflow (e.g., net exfiltration from sewer lines, wastewater effluents, and lawn irrigation) may mask or confound fundamental changes in hydrologic pathways on a case-specific basis (Lerner 2002). Notwithstanding the potential for site-specific confounding variables, baseflow reduction due to urbanization has been cited in recent total maximum daily load (TMDL) studies as a significant stressor (MDEP 2006; VTDEC 2006; VTDEC 2009) contributing to water quality and aquatic life impairments.

As set forth by the National Research Council (NRC 2008), the use of streamflow volume or impervious cover may be a useful TMDL surrogate where unknown agents or processes are causing freshwater impairment. Volume-based flow reduction TMDLs provide an example of a growing trend in which changes in hydrologic response or streamflow alteration, including assumed baseflow reductions, have been cited as an aquatic life stressor (U.S. EPA 2011). In addition to changes in flow regime, TMDL documents often provide a suite of other possible aquatic life stressors including (but not limited to) narrow riparian corridors, warmer water temperatures, toxic contaminants, increased sedimentation, and stream channel scour (U.S. EPA 2011). Detailed hydrologic analyses are needed to more clearly identify urban hydrological, water quality, and biological stressors. Improved understanding will result in greater certainty and successful outcomes of pollution control measures [e.g., source or transport interruption, and best management practices (BMPs) (Mostaghimi et al. 2001; Pazwash 2011].

Separating groundwater flow from quick flow contributions to measured streamflow time series has been achieved using several methods including traditional graphical analyses (Barnes 1939), isotopic analyses (Ellins et al. 1990; Genereux and Hooper 1998; Tetzlaff and Soulsby 2008), geochemical or in situ chemical signatures (Newbury et al. 1969; Wels et al. 1991; Kish et al. 2010), various analytical methods (Brutsaert and Nieber 1977; Birtles 1978), and automated algorithms applied to streamflow time series (Nathan and McMahon 1990; Chapman 1999; Eckhardt 2008). Automated methods of baseflow computation were recently applied by Meyer (Meyer 2005), Brandes et al. (Brandes et al. 2005), and Esralew and Lewis (Esralew and Lewis 2010) to evaluate streamflow metric trends within a variety of land uses, aquifer types, and stream connectivity scenarios. Application of automated separation algorithms typically proceeds following calibration to presumed baseflows supported by recession analysis (Tallaksen 1995). Selecting the location where baseflow dominates the hydrograph is often a confounding process (Vogel and Kroll 1996). Sujono et al. (Sujono et al. 2004) indicated that a more objective method of wavelet transform appears promising. Once properly parameterized, automated methods are widely accepted to be more objective and reproducible (Nathan and McMahon 1990; Arnold and Allen 1999; Furey and Gupta 2001) and therefore preferable over more subjective graphical methods. In addition to algorithm structure, the timing and magnitude of precipitation is a key determinant and uncertainty in evaluating hydrologic response.

The relationship between precipitation input and catchment response was described by several researchers as nonlinear resulting from partial source behavior, seasonal changes in soil moisture, event magnitude, spatial scale, preferential flow paths, and saturation excess frequencies (Goodrich et al. 1997; Kokkonen et al. 2004; Kusumastuti et al. 2007; McDonnell et al. 2007; McGrath et al. 2007). Quantifying changes in hydrologic response solely attributable to time should therefore also consider and adjust for effects induced by precipitation inputs. Recent baseflow trend analyses performed by Brandes et al. (Brandes et al. 2005) and Esralew and Lewis (Esralew and Lewis 2010) addressed precipitation effects through normalization or adjustment by residual.

Helsel and Hirsch (Helsel and Hirsch 2002) described a two-step residual analysis approach to adjust for precipitation effects. The two-step approach can be selected over the one-step multiple regression approach described by Helsel and Hirsch (Helsel and Hirsch 2002) to support graphical depiction and improve understanding of the effect of precipitation on trend slopes and time series variability. In the absence of calibration to more direct tracer-derived estimates of baseflow (e.g., Gonzales et al. 2009), algorithm parameters remain constrained to a range of values cited in the literature. Propagating parameter uncertainty into streamflow metric estimates and trend determinations can be facilitated by Monte Carlo techniques. Instead of deriving streamflow metrics with a single set of base case or "best estimate" of baseflow separation parameters, Monte Carlo techniques specify algorithm inputs as random numbers generated from prescribed statistical distributions

(Morgan and Henrion 2003). Application of Monte Carlo analyses to constrain and thus better understand uncertainties in hydrologic analyses was discussed or used by several authors, including Smith and Hebbert (Smith and Hebbert 1979), Beven (Beven 1993), Beven and Freer (Beven and Freer 2001), and Peters and van Lanen (Peters and van Lanen 2005).

The overarching objective of the following work was to evaluate three sources of uncertainty in annual hydrologic trend analyses in a central U.S. case study: nonlinear precipitation effects, structure of baseflow separation algorithm, and parameter variability. To achieve these objectives, we employed two dissimilar baseflow separation techniques using data collected in a representative urban watershed in the central United States. The first separation technique was a two-parameter recursive filter derived by Eckhardt (Eckhardt 2005) and the second was a two-parameter algorithm proposed by Wittenberg (Wittenberg 1999) that assumes a nonlinear aquifer storage–outflow relationship. Trends, behavior, and uncertainty of hydrologic response predicted by these two algorithms are described. The working assumption was that an analysis considering the uncertainties referenced above will improve our ability to identify streamflow alteration over time, thereby quantitatively supporting development decisions and science-based policy.

2. Materials and methods

2.1. Study site

Information required to fulfill the objectives of this work were supplied by means of a case study analysis in the Hinkson Creek watershed (HCW) located within the lower Missouri–Moreau River basin (LMMRB) in central Missouri (Figure 1 and Table 1). Hinkson Creek flows through a catchment basin of approximately 231 km^2. The creek flows approximately 42 km in a southwesterly direction ultimately flowing into the Missouri River approximately 8 miles away. Elevation ranges from 177 to 274 m above mean sea level (MSL) in the headwaters. Hinkson Creek is classified as a Missouri Ozark border stream located in the transitional zone between glaciated plains and Ozark natural divisions (Thom and Wilson 1980). Average annual temperature and precipitation (30-yr record) are approximately 14°C and 1082 mm, respectively. The HCW is a representative urban watershed given its growing residential composition (ca. 108 500 residents) with progressive commercial expansion. Current land use in the watershed is approximately 34% forest; 38% pasture or cropland; 25% urban area; and the remaining land area is wetland, open, or shrub/grassland areas. A U.S. Geological Survey (USGS) gauging station (USGS 06910230) has collected stage data intermittently in the HCW since 1966 (Figure 1).

Soil types range from loamy till with a well-developed clay pan in the uplands (Chapman et al. 2002) to thin cherty clay and silty to sandy clay in lower reaches. Soils are generally underlain by Mississippian series limestones (Burlington formation) and Pennsylvanian series sandstones (Cherokee group) (Unklesbay 1952; Miller and Vandike 1997). Lithology of the Burlington formation is white to tan fossiliferous limestone having layered chert nodules, whereas the Cherokee group is a mix of sandstone, shale, underclay, and thin limestone beds (Miller and Vandike

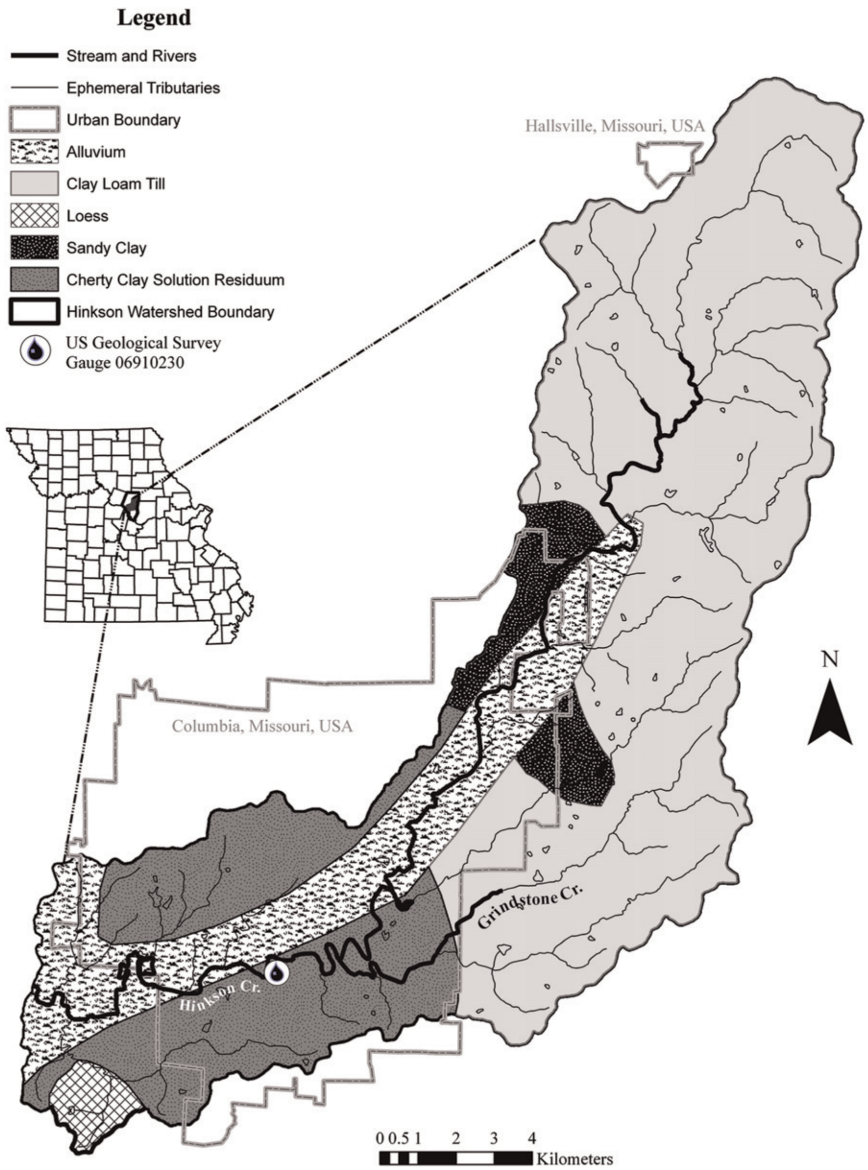

Figure 1. The Hinkson Creek watershed located in central Missouri.

1997). Mississippian limestones are estimated to directly underlay 40% (91 km^2) of HCW soils and are located primarily near the watershed outlet (Starbuck 2007; Figure 1). Hinkson Creek intermittently flows over bedrock outcroppings throughout its course and is frequently bounded by floodplains composed of Haymond silt loams (Unklesbay 1952; Young et al. 2001). Surficial geology near the USGS gauge 06910230 is a cherty clay solution residuum often corresponding to the Weller–Bardley–Clinkenbeard (CBC) association (USGS 1996; Young et al. 2001). Although karst features have not been well documented in lower Hinkson Creek, the CBC association is linked with sinkholes and caves in the adjacent

Table 1. Characteristics of the Hinkson Creek watershed located in central Missouri.

Characteristic	Description
USGS gauge 06910230	Location: 38°55′39.9″N, 92°20′23.8″W
	Datum elevation: 177.9 m MSL
	Period of record: $n = 22$ calendar years
	1967–81
	1987–90
	2008–10
	Mean annual: 1.75 $m^3 s^{-1}$ (CV = 0.71)
	Flow: 0.83 mm day^{-1}
Watershed area	Total: 231 km^2; Upstream of gauge: 181 km^2
Quaternary geology (upstream of gauge) (USGS 1996)	Clay loam till (74%)
	Alluvium (11%)
	Sandy clay (6%)
	Thin cherty clay (8%)
	Solution residuum
Surface bedrock	Mississippian limestone (40%)
	Pennsylvanian sandstone (60%)
2006 land cover	Row crop (8%)
	Grassland/pasture (30%)
	Urban (26%)
	Forest (34%)
	Other (2%)

Bonne Femme watershed located to the southeast of the HCW (Wicks 1997; Lerch et al. 2005).

2.2. Precipitation

Hydroclimate data from two nearby climate stations (231790 and 231791) catalogued by the Midwest Regional Climatic Center (MRCC 2010) were used to assess temporal changes in hydrologic response and selection of streamflow recession segments for the HCW. Station 231790 representing precipitation for the 1966–69 period was located approximately 5.1 km northwest of the Hinkson Creek USGS gauge and within the footprint of the historic Columbia Municipal Airport. Data from 1969 through 2010 was measured at station 231791, the current location of the Columbia Regional Airport, located 16.3 km to the southeast of the Hinkson Creek USGS gauge (Figure 1).

2.3. Land use and population

Human population data since 1970 for the city of Columbia and Boone County, Missouri, areas were queried from U.S. Census Bureau databases. Four land-use and land-cover (LULC) geospatial datasets were used in assessing changes in urban land use with time. The earliest is a 1976 layer (Harlan 1997) developed from land-surveyor notes developed by the U.S. Geological Survey that classifies LULC at the level II scale of Anderson et al. (Anderson et al. 1976). Three Landsat Thematic Mapper (TM) datasets for periods of 1991–93, 2000–04, and circa 2006 were used to estimate recent land-use changes. Land-cover classifications differ

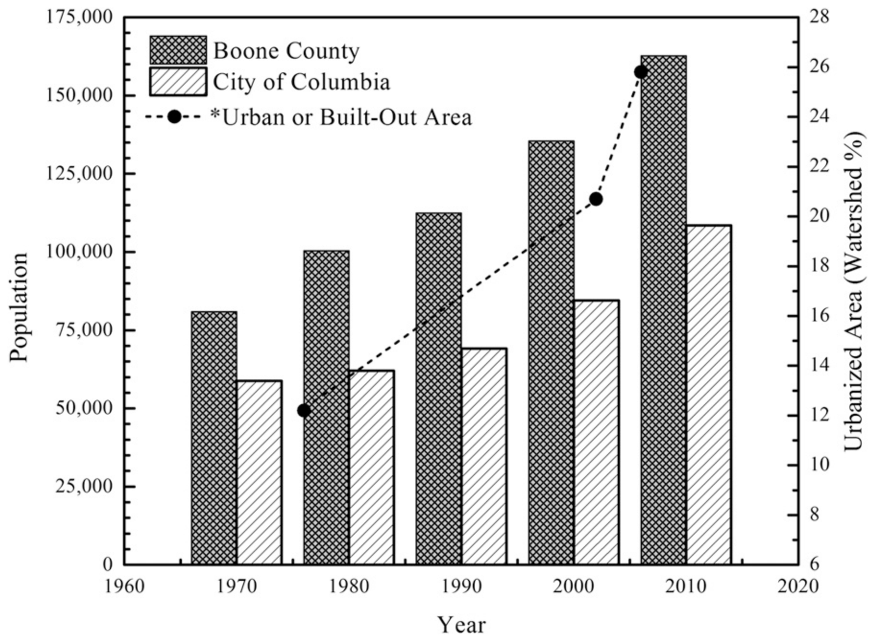

Figure 2. Population and urbanized area of the Hinkson creek watershed located in central Missouri from 1960 to 2010. The urbanized area estimated from 1993 land-use classification is not shown as areas identified as grassland or pasture in 1993 are subsequently categorized as low density urban in later coverages.

among available TM coverages. In an attempt to compare like classifications, urban land-use changes were grouped into one category identified here as urban/built out (UBO). Land uses described by UBO include urban impervious (nonvegetated), high building density urban (some vegetation, majority as imperviousness), and low building density (residential and developed open space) with moderate vegetation.

The population of Boone County increased from 80 911 in 1970 to 162 642 in 2010 (Figure 2). During the same period, the population of the city of Columbia grew from 58 812 to 108 500. Expressed as a percentage of the entire HCW area, UBO has increased from approximately 12% in 1976 to 26% in 2006. Given alternative LULC classifications and uncertainty, we estimate current (2006 LULC) impervious area (IA) is approximately 10% in the HCW as described by the sum of high and medium density urban classifications and visual confirmation using high-resolution aerial photography. While researchers have linked IA with aquatic degradation (see review by Booth et al. 2002), Jones et al. (Jones et al. 2005) emphasized that IA is a broad indicator of pollution potential and relationships to biologic integrity are uncertain. In this work, our estimate of IA in the HCW is provided only as means of comparison to other urbanizing catchments.

2.4. Baseflow separation and parameterization

Selection and parameterization of automated baseflow methods require selection of an aquifer storage–discharge model (e.g., linear, nonlinear), a consistent means of criteria for parsing recession limbs, a procedure for quantifying recession parameters, and numerical methods necessary to apply the algorithm to a specific streamflow time series (Moore 1997; Rutledge 1998; Sujono et al. 2004; Tallaksen 1995). Selections for this work are detailed in the following paragraphs. Separation algorithms and Monte Carlo analyses were implemented in Microsoft Excel and, where necessary, programmed in Visual Basic language.

The Eckhardt (Eckhardt 2005) separation method [Equation (1)] is a recursive low-pass digital filter that Eckhardt (Eckhardt 2008) described as including the assumption of a linear storage–outflow relationship [Equations (2) and (4)],

$$b_t = \frac{(1 - \mathrm{BFI}_{\max})kb_{t-1} + (1 - k)\mathrm{BFI}_{\max}y_t}{1 - k\mathrm{BFI}_{\max}}, \tag{1}$$

where b_t is the baseflow at time step t, $\mathrm{BFI}_{\max}$ is the maximum rate of baseflow relative to streamflow if time series magnitude remains constant, k is the baseflow recession constant, b_{t-1} is the baseflow at time step $t - 1$, and y_t is the measured streamflow at time step t. Note that b_t is subject to the Boolean constraint of $b_t \leq y_t$. The recession constant k is widely used in recession analysis to describe the slope between adjacent streamflows. According to Maillet (Maillet 1905) and described by several others (Tallaksen 1995; Chapman 1999; Sujono et al. 2004; Eckhardt 2008), streamflow that consists entirely of baseflow following a recharge event can be described by

$$b_t = \mathrm{b}_0 \exp^{-(t/\tau)} = b_0 k^t, \tag{2}$$

where b_0 is the initial streamflow at the beginning of baseflow recession and τ is the groundwater residence time, which is interpreted as the inverse ratio of storage to outflow in a linear reservoir in

$$b = \frac{1}{\tau} = aS, \tag{3}$$

where S is the groundwater storage and $a = 1/\tau$. The recession constant k has been determined by a variety of methods (e.g., Tallaksen 1995; Sujono et al. 2004). In this analysis, we used the correlation method described by Eckhardt (Eckhardt 2008) to obtain $k = 0.965$ from the envelope line of a master recession curve (Figure 3) with a lag interval of 1 day. The resulting master recession curve shows a total of 24 recession segments identified in the streamflow time series with a minimum length of 10 days (Nathan and McMahon 1990; Vogel and Kroll 1996; Arnold and Allen 1999) and beginning no less than 2 days following the hydrograph peak. Precipitation was accounted for as per Furey and Gupta (Furey and Gupta 2001). The $\mathrm{BFI}_{\max}$ parameter is presumably related to area-weighted average aquifer characteristics, where $\mathrm{BFI}_{\max} = 0.8$ for perennial streams with porous aquifers, $\mathrm{BFI}_{\max} = 0.5$ for ephemeral streams with porous aquifers, and $\mathrm{BFI}_{\max} = 0.25$ for perennial streams with hard-rock aquifers (Eckhardt 2008). A stream is considered ephemeral if measurable surface flow is absent less than 10% of the time (Eckhardt 2008). On this basis, Hinkson Creek was considered a perennial stream (10th percentile $y_t = 0.01\ \mathrm{m^3\,s^{-1}}$). While use of tracers to calibrate separation parameters is desirable (see Gonzales et al. 2009), such data are often

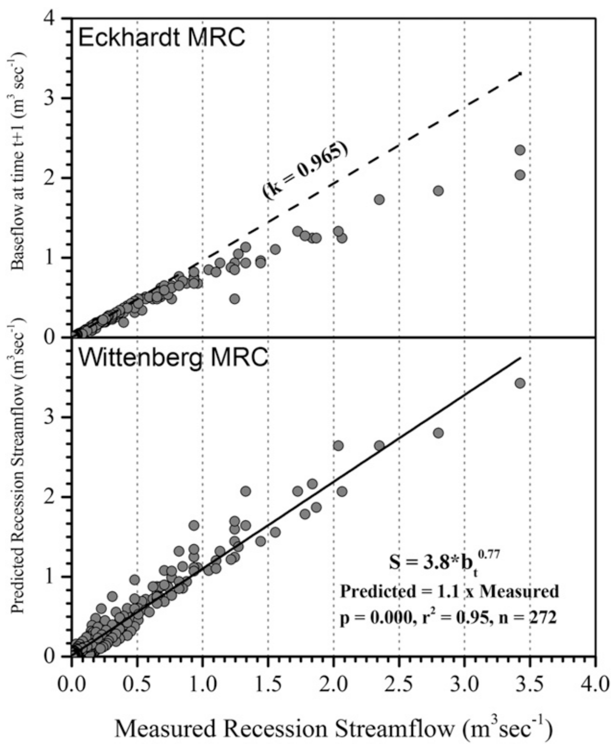

Figure 3. Master recession curves derived using correlation methods for Hinkson Creek located in central Missouri, 1966–2010 (*n* = 24 recession segments; 248 correlations).

absent, leaving determination of baseflow parameters or metrics dependent on the weight of evidence and/or geologic interpretation (e.g., Bloomfield et al. 2009). Derivation of BFI_{max} within a heterogeneous geologic setting such as the HCW is challenged by higher yield of carbonate hard-rock aquifers in lower reaches near the USGS gauge that were associated with fast-response and conduit characteristics of karst (Padilla et al. 1994; Lerch et al. 2005). In contrast to the geology of the Burlington formation, Pennsylvanian sandstones (well yield = 3.8–76 L min^{-1}; Miller and Vandike 1997) overlaid by clay loam till exhibit moderate to low permeabilities ($K = 10^{-11}$ to 10^{-7} m s^{-1}; Sharp 1984) throughout middle and upper reaches (with some exceptions) of the HCW. An areal-weighted BFI_{max} value of 0.62 (0.5 × 60% + 0.8 × 40%) was reasoned by assuming a 0.5 value for 60% of the HCW and an intermittent stream course underlaid by Pennsylvanian sandstone and limestone. The remainder of the catchment (40%) where soils are underlaid primarily by the Burlington formation (yield = 57–1893 L min^{-1}; Miller and Vandike 1997) was assumed to have a porous aquifer value of 0.8 justified by karstic associations (Wicks 1997). A weighted BFI_{max} = 0.62 produced baseflow time series having realistic appearance during a typical recession season (summer) hydrograph (Figure 4).

Increases in the calculated recession constant *k* [Equation (2)] with time along the recession (an indication of nonlinearity) were noted by several authors (Vogel

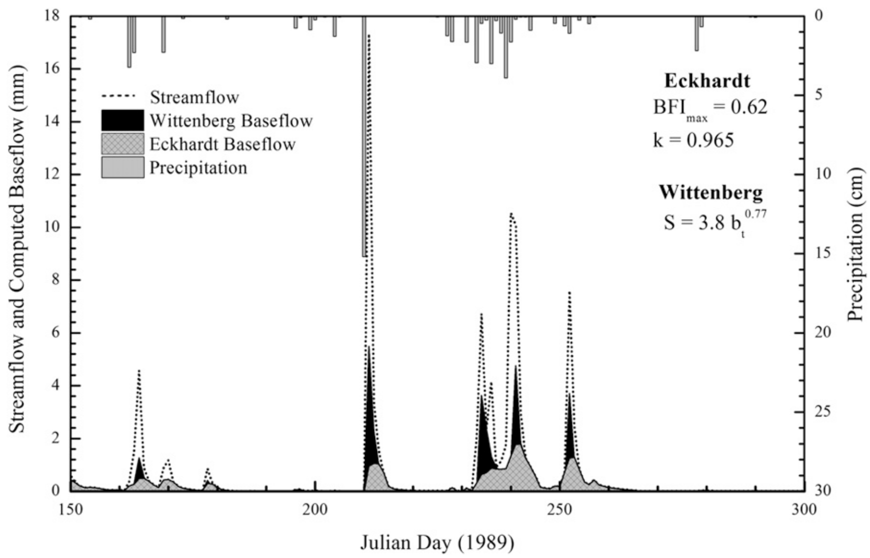

Figure 4. Streamflow and computed baseflow during the 1989 summer recession period for Hinkson Creek located in central Missouri.

and Kroll 1996; Moore 1997; Wittenberg 1999; Furey and Gupta 2001). As systematic increases in k were also observed in several Hinkson Creek recessions, a baseflow separation algorithm incorporating a nonlinear storage–outflow relationship was applied in addition to the Eckhardt (Eckhardt 2005) filter.

Wittenberg (Wittenberg 1999) proposed a nonlinear separation algorithm [Equation (4)] that is applied backward in time as

$$b_{t-1} = \left[b_t^{\beta-1} + \frac{\Delta t(\beta - 1)}{\alpha\beta}\right]^{(1/\beta-1)}, \tag{4}$$

where β and α are the exponent and coefficient, respectively, of the nonlinear storage relationship [Equation (5)] credited to Coutagne (Coutagne 1948),

$$S = \alpha b_t^{\beta}. \tag{5}$$

Application of Equation (4) to streamflow time series requires two Boolean conditions. The first addresses the situation when backward computed recession limbs intercept the rising limb of hydrographs. For time steps where baseflow exceeds total streamflow during recharge events, the baseflow hydrograph is calculated as one time step into the future using the forward-difference [Equation (6)] version of Equation (4),

$$b_t = b_0\left[1 + \frac{b_0^{1-\beta}(1 - \beta)}{\alpha\beta}t\right]^{(1/\beta-1)}. \tag{6}$$

As nonlinear storage parameters α and β are stationary, individual recessions where baseflow computed with Equation (4) is greater than total streamflow are unavoidable. Therefore, as with the Eckhardt filter, the Boolean constraint of $b_t \leq y_t$ was forced.

Acceptable fit of separation parameters $\alpha = 3.80$ and $\beta = 0.77$ was obtained through least squares optimization of computed and measured recession outflow volumes according to Equation (7) as used by Wittenberg (Wittenberg 1999),

$$\alpha = \frac{\sum (b_{t-1} + b_t)\Delta t}{2\sum (b_{t-1}^{\beta} - b_t^{\beta})}. \tag{7}$$

Parameter estimation [root-mean-square error (RMSE) = 0.14, $r^2 = 0.95$, and $n = 272$] fit was quantified by comparison of measured and computed baseflow rates (Figure 4) according to the forward nonlinear recession [Equation (6)] using $\alpha = 3.80$ and $\beta = 0.77$. A value of $\beta > 0.5$ suggests that macropores (Wittenberg 1999), possibly related to karst development, may be influencing recession behavior. Nonlinear storage parameters α and β are values derived from recession limbs pooled over high and low evapotranspiration seasons and were not derived separately by season (e.g., Wittenberg 2003).

Effective groundwater recharge (GWRE) (Chapman 1999; Wittenberg 2003) was computed from both algorithms according to Equation (8) to assess the reasonableness of computed baseflows,

$$\mathrm{GWRE}_t = S_t - S_{t-1} + \int_{\mathrm{t}-1}^{t} (b)\, dt \tag{8}$$

where S_t and S_{t-1} are groundwater storage at times t and $t - 1$ computed with Equations (3) and (5). Equation (8) can be further expanded (see Wittenberg 2003) to explicitly include groundwater abstractions (A) and evapotranspiration (ET) as

$$\mathrm{GWRE}_t = S_t - S_{t-1} + \int_{t-1}^{t} (b + A + \mathrm{ET})\, dt. \tag{9}$$

2.5. Streamflow variables and statistical analyses

Annual (January–December) hydrograph characteristics evaluated to detect urbanization effects in the HCW included baseflow and runoff volumes, the runoff coefficient (event runoff/precipitation), baseflow index (BFI; baseflow volume/streamflow volume), baseflow yield (baseflow volume/precipitation volume), and effective groundwater recharge (as per Spinello and Simmons 1992; Rose and Peters 2001; Wittenberg 2003; Brandes et al. 2005; Meyer 2005).

Monotonic changes in precipitation and computed baseflow and runoff statistics with respect to time were evaluated using the Mann–Kendall test (Hirsch et al. 1991). The Mann–Kendall S test is a nonparametric measure of monotonic trend that is resistant to outliers or skew (Helsel and Hirsch 2002). The Kendall S is related to the tau-b correlation coefficient τ that falls within a range of 1.0 to -1.0 reflecting a perfect positive and negative monotonic trend, respectively (Helsel and Hirsch 2002). Two-tailed tests of the null hypothesis H_0 (trend absent) using the S

statistic (adjusted for ties) were conducted at $\alpha = 0.05$ or 95% confidence to identify trends ($p \leq 0.05$). Where significant trends were detected, the monotonic slope of the relation was provided as the Kendall–Theil T robust line (Conover 1980). In this work, τ was used more frequently than S because the operational range (1.0 to -1.0) is analogous to the commonly used Pearson's r. The tau-b correlation statistic was used to describe several relationships in this work including the following: precipitation versus streamflow metric, parameter sensitivity, and streamflow metric versus time. In addition, streamflow metric differences between baseflow separation method were tested pairwise where possible using the Wilcoxon signed-rank test (Helsel and Hirsch 2002).

The influence of exogenous variables, such as precipitation, has been reported by others conducting baseflow time trend analyses (Brandes et al. 2005; Esralew and Lewis 2010). Removal of exogenous effects, termed adjustment, was considered if a significant ($p \leq 0.05$) correlation between a streamflow metric and precipitation was detected according to Kendall's tau-b coefficient and, for comparison, the more familiar Pearson's linear r correlation coefficient. The purpose of adjustment was to better isolate changes in streamflow metrics due to time, rather than changes in a significant covariate(s) over time. If significant exogenous influence was detected, analyses proceeded in two steps described in Helsel and Hirsch (Helsel and Hirsch 2002): 1) regress streamflow metric against precipitation using locally weighted scatterplot smoothing (LOWESS) (Cleveland and Devlin 1988) technique and then 2) conduct a Mann–Kendall hypothesis test on the LOWESS error residuals and time to identify temporal trends.

2.6. Baseflow separation algorithm performance and sensitivity

Two algorithm performance metrics were adopted for this evaluation. The first was proposed by Furey and Gupta (Furey and Gupta 2001) and includes the percent of time that predicted baseflow exceeds total streamflow π_1. This metric was also used by Peters and van Lanen (Peters and van Lanen 2005). As noted in the previous section, Boolean contraints were imposed on both algorithms to prevent predicted baseflow from exceeding streamflow. While this physical constraint is useful in deriving base-case streamflow metrics, it restricts parameter assessment. Therefore, performance metrics were implemented on time series not subject to the Boolean constraint, termed unconstrained baseflow, for each algorithm. A second performance metric π_2 included comparison [as RMSE: Equation (10)] of unconstrained baseflow to total streamflow values occurring 10 days or more following initiation of recession [target recession values (TRVs)] during $n = 24$ selected limbs previously described. In selecting these TRVs, the intent was to minimize the influence of interflow in evaluating performance of baseflow algorithms,

$$\mathrm{RMSE} = \sqrt{\frac{1}{n}\sum_{i=1}^{n}(b_m - b_p)^2}\,, \tag{10}$$

where b_m is the streamflow measured during recession (assumed 100% baseflow) and b_p is the unconstrained baseflow predicted by the algorithm. Sensitivity of

Table 2. Monte Carlo input parameter ranges, distributions, and best parameter sets. The term μ is the mean, and σ is the parameter standard deviation, approximated as ASE.

Baseflow algorithm parameters	Distribution	Initial distribution parameters	Best parameter sets		
			π_1	π_2	
			min = 0.930	min = 0.93	min = 0.93
	k	Uniform	max = 0.995	max = 0.96	max = 0.95
			min = 0.25	min = 0.25	min = 0.25
Eckhardt	BFI_{max}	Uniform	max = 0.80	max = 0.35	max = 0.80
			μ = 3.80	min = 2.74	min = 4.21
	α	Normal	σ = 0.333	max = 3.62	max = 5.04
			μ = 0.77	min = 0.71	min = 0.68
Wittenberg	β	Normal	σ = 0.031	max = 0.89	max = 0.84

streamflow metrics to algorithm parameters were assessed as per Kendall's tau-b, a nonparametric correlation measure previously described.

2.7. Monte Carlo simulation and parameterization

The Monte Carlo software add-in Yet Another Software Add-In, version W (YASAIW; Pelletier 2009) was used to generate random baseflow algorithm parameters and store propagated estimates of annual streamflow metrics. Precipitation adjusted and unadjusted nonparametric time trends (as Kendall's tau-b) were calculated from annual streamflow metrics during Monte Carlo iterations. Values of tau-b generated at each iteration were stored in memory allowing a trend hypothesis test be conducted for each of $n = 2000$ iterations. In addition to tau-b, algorithm parameters, streamflow metrics, LOWESS predictions, and residuals were stored to supply necessary modeling inputs for later algorithm sensitivity analyses. Algorithm performance metrics previously described were also stored in memory from each modeling run. Statistical distributions and parameters needed for Monte Carlo inputs are described in the following paragraphs.

The Eckhardt (Eckhardt 2005) filter is described by two parameters: the baseflow recession constant k and BFI_{max}. Eckhardt parameters are discussed in referenced order. As summarized by Nathan and McMahon (Nathan and McMahon 1990), streamflow recession rates attributable to baseflow typically range from 0.93 to 0.995, while interflow k values (0.70–0.94) slightly overlap baseflow at higher recession rates. In an analysis of 23 sites in Massachusetts, Vogel and Kroll (Vogel and Kroll 1996) estimated the long-term k to range from 0.86 to 0.96 using six different recession constant estimators. In the absence of a range of k values determined for Missouri or site-specific direct tracer measurements, k was randomly selected from a uniform distribution and constrained to a range of 0.93–0.995 (Table 2). The BFI_{max} parameter is not physically based but rather an a priori estimate of the long-term baseflow proportion of total streamflow (Eckhardt 2008). Notwithstanding the $BFI_{max} = 0.92$ derived through calibration to geochemical tracers by Gonzales et al. (Gonzales et al. 2009), we selected BFI_{max} from a uniform distribution within the potential range of 0.25–0.80 described by Eckhardt (Eckhardt 2008).

Parameters β and α of the Wittenberg (Wittenberg 1999) algorithm were determined through nonlinear least squares regression using the System Statistics

(SYSTAT) 11 platform. With this approach, we employed uncertainty bounds for β and α parameters (Table 2) presuming asymptotic normality (Bates and Watts 1988). For the current analysis, the 95% asymptotic confidence interval around β (0.77 ± 0.062) and α (3.8 ± 0.666) were adopted and described by asymptotic standard errors (ASE) of 0.031 and 0.333, respectively (Table 2).

3. Results and discussion

3.1. Precipitation

Precipitation during the period of analysis varied from 601 mm (1981) to 1583 mm (1993). Cumulative annual precipitation measured at station 231791 did not exhibit a significant monotonic two-sided time trend ($S = 102$, $p = 0.307$, and $n = 44$) during the 1967–2010 period. However, precipitation was significantly ($p \leq 0.05$) correlated to all streamflow metric trend analyses. With the exception of the Eckhardt BFI ($r^2 = 0.34$), precipitation explained greater than 50% of the variation ($r^2 > 0.5$) in annual streamflow metrics.

Nonlinear relationships between precipitation inputs and annual LOWESS streamflow metrics were evident in results, with the exception of BFI (Figure 5). Annual streamflow metrics yielded by precipitation inputs tended to increase in the range of 900–1000-mm (change point) annual cumulative precipitation. The physical basis for nonlinear behavior including (but not limited to) saturation excess frequencies, soil macropore activity, or event magnitude were expressed by several authors (Goodrich et al. 1997; Kokkonen et al. 2004; Kusumastuti et al. 2007; McDonnell et al. 2007; McGrath et al. 2007). Quantifying the causes or mechanisms of nonlinear behavior in the HCW is beyond on the scope of the current work. However, the observed nonlinear relationships and change points detected by both algorithms underscore the dependence of streamflow metrics on precipitation inputs. To quantify changes in streamflow metrics attributable to factors other than precipitation, such as time, we removed the exogenous effects of water inputs from HCW time series. The inference being that temporal changes in precipitation adjusted time series could reflect effects of urbanization.

3.2. Algorithm performance and parameter sensitivity

The Wittenberg algorithm performed better than the Eckhardt filter across perturbed parameter ranges during $n = 2000$ iterations. The overprediction frequency π_1 for the Wittenberg algorithm [median $\pi_1 = 14.8\%$; interquartile range (IQR) = 14.6%–15.0%] was significantly less ($p \leq 0.05$) than produced by the Eckhardt filter (median $\pi_1 = 64.4\%$; IQR = 58.5%–69.4%). The RMSE π_2 produced by the two algorithms for $n = 56$ TRVs was significantly less ($p \leq 0.05$) for the Wittenberg algorithm (median RMSE = 0.013 mm day^{-1}; IQR = 0.012–0.014 mm day^{-1}) than the Eckhardt filter (median RMSE = 0.299 mm day^{-1}; IQR = 0.225–0.418 mm day^{-1}). While the Wittenberg outperformed the Eckhardt filter in this analysis, the model does not explicitly address all uncertainties related to karst features. There is currently no direct evidence of such features in the study watershed; however, the question provides impetus for future investigations. The

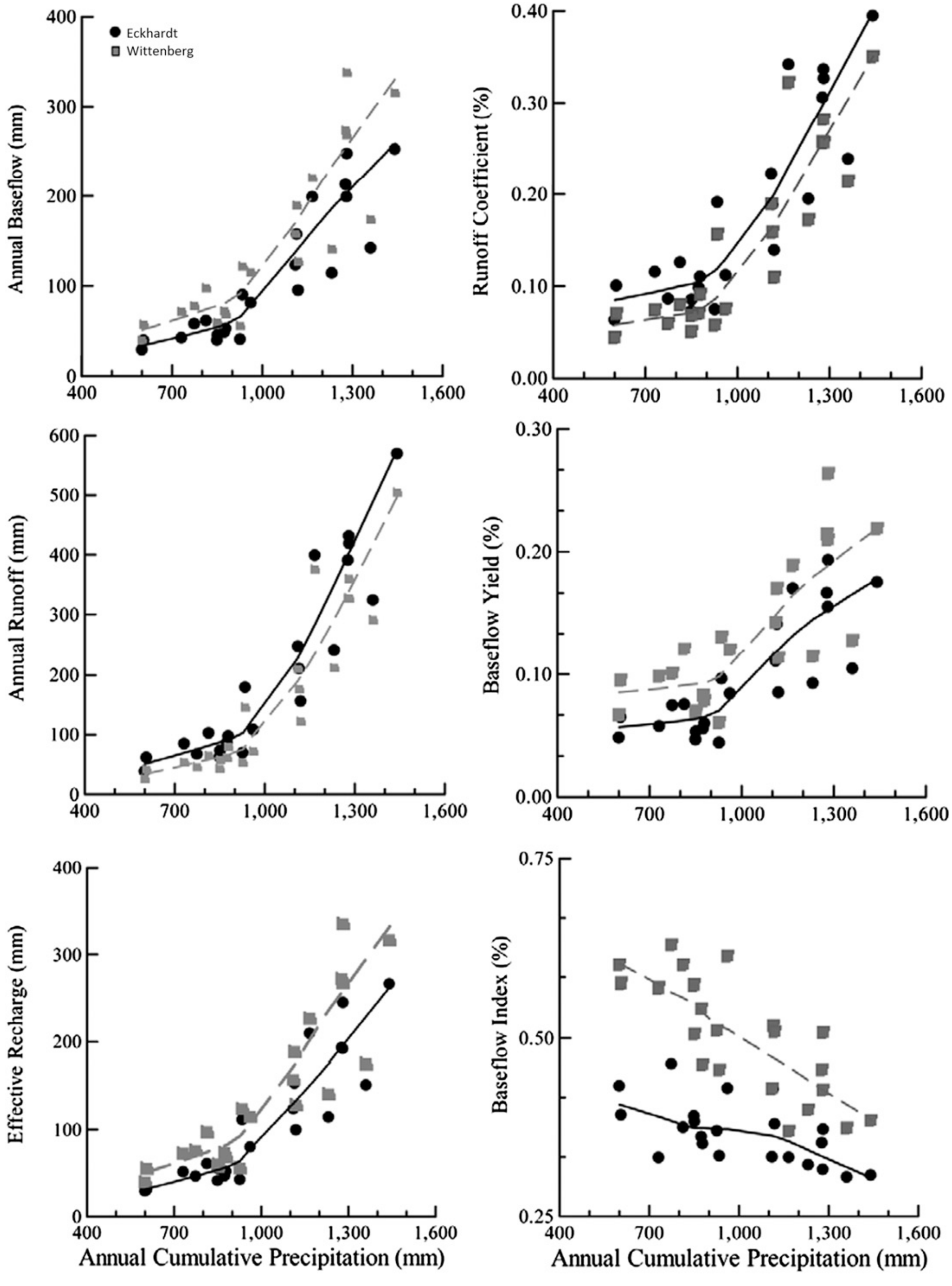

Figure 5. Relationships depicted by LOWESS between Annual precipitation and streamflow metrics calculated from base-case Eckhardt (black) and Wittenberg (gray) separation algorithms for Hinkson Creek gauge 06910230 (1967–2010; n = 22 comparisons) located in central Missouri.

RMSE π_2 was most sensitive to the recession constant (k tau-b = 0.69; BFI_{max} tau-b = 0.24) for the Eckhardt filter and to α (α tau-b = −0.88, β tau-b = 0.11) in the Wittenberg algorithm.

The superior performance of the Wittenberg algorithm for estimating baseflows in the HCW time series is attributed to algorithm structure and parameterization methodology. The Eckhardt method uses a recession constant derived from a master recession curve, limited to a range of 0.93–0.995 in Monte Carlo simulations, and BFI_{max} subjectively related to an aquifer–stream relationship. Wittenberg parameters (α and β) are calculated directly from observed streamflow time series via least squares nonlinear regression. On this basis, we propose that improvements of Eckhardt algorithm performance metrics could be achieved by using nonlinear regression to determine k and BFI_{max} (e.g., Vogel and Kroll 1996; Chapman 1999).

Acceptable input ranges useful in future studies may be evaluated through inspection of parameters sets yielding the lowest values of π_1 and π_2. In this evaluation, the lowest (i.e., best) 5% from Monte Carlo iterations (Peters and van Lanen 2005) revealed that best parameter sets differed by performance metric (Table 2). For example, the value of α yielding the lowest π_1 values ranged from 2.7 to 3.6 (median = 3.2), whereas minimizing π_2 yielded a range of 4.2–5.0 (median = 4.4). Differences of BFI_{max} were more severe, with π_1 minimized values ranging from 0.25 to 0.35 (median = 0.28) compared to π_2 minimized values of 0.25–0.80 (median = 0.71). These divergent sensitivities suggest that a more robust suite of performance metrics or fitness measures should be developed to evaluate algorithm performance.

3.3. Long-term hydrologic response

Median annual streamflow (220 mm; $n = 22$ years) recorded at gauge 06910230 (USGS site) in the HCW was estimated to be 23% of median annual precipitation (949 mm; $n = 22$) during comparable periods of record, suggesting an annual surface water balance dominated by the ET processes. Median annual baseflow (Table 3) differed by algorithm ($p \leq 0.05$), with the Eckhardt equation (85.3 mm yr^{-1}) predicting 29% less volume than Wittenberg (118.9 mm yr^{-1}). This difference predictably propagated to residual metrics calculated from baseflow predictions. That is, the Eckhardt algorithm predicted relatively lower baseflow metrics and therefore greater runoff compared to the Wittenberg method. Long-term baseflow and runoff computed by each algorithm were significantly different at $p \leq 0.05$ for base-case estimates (Table 3) and Monte Carlo simulations (Figure 6). Long-term medians produced from Wittenberg Monte Carlo simulations did not differ from base-case values. Greater parameter uncertainty of the Eckhardt algorithm resulted in Monte Carlo analysis generating a lower annual BFI (0.32) and higher RC (0.14) than base-case values. Density functions produced by each algorithm are useful in describing hydrologic response metrics (Figure 6).

The variance and shape of long-term streamflow metric distributions of each algorithm were markedly different (Figure 6) and thus emphasize the effect of algorithm structure on hydrologic response. Wittenberg metrics were significantly less variable; kurtotic; and, in the case of runoff metrics, bimodal. Bimodal

Table 3. Annual base-case streamflow metrics calculated with Eckhardt and Wittenberg algorithms for gauge 06910230 (1967–2010; $n = 22$ comparisons) located in Columbia, Missouri.

Streamflow metric	Eckhardt Median*	Eckhardt IQR**	Wittenberg Median*	Wittenberg IQR**
Baseflow volume (mm)	85.3	153.3–46.0	118.9	185.0–69.7
Runoff volume (mm)	131.6	304.4–75.6	101.6	272.0–55.4
Effective recharge (mm)	89.6	47.7–152.0	120	70.1–185.5
Runoff coefficient (%)	0.13	0.23–0.10	0.1	0.21–0.07
Baseflow index (%)	0.37	0.39–0.33	0.51	0.57–0.44
Baseflow yield (%)	0.08	0.13–0.06	0.12	0.16–0.09

* Wilcoxon $Z_{sr} = \pm 4.11$ ($p \leq 0.00$; $n = 22$; large sample approximation).

** The interquartile range is 75th–25th percentile.

elevated runoff response was produced by infrequent predictions of reduced baseflow that occurred when α was low, β was high, and they were not constrained by Boolean (forward recession) truncation. Median annual hydrologic response produced by the Wittenberg algorithm was considerably less sensitive to parameter variability ($|\text{tau-b}| \leq 0.29$) compared to Eckhardt algorithms ($|\text{tau-b}| = 0.16$–0.84) (Table 4). This reduced sensitivity is the result of α and β switching correlation signs ($+$ to $-$ and $-$ to $+$) during backward to forward computed recessions. For example, during periods when recessions are computed backward and do not exceed streamflow (i.e., long recession periods), α is negatively correlated and β is positively correlated with computed baseflow. When backward predicted baseflow exceeds streamflow, baseflow is computed as a forward recession. Parameters α and β switch signs during forward recessions resulting in positive and negative correlations, respectively. The duration and frequency of unconstrained predicted baseflows lead to net correlations listed in Table 4: several of which feature tau-b values near zero. Changes in correlation sign during backward and forward application of the nonlinear Wittenberg algorithm appear to serve as a buffer against parameter uncertainty.

Eckhardt algorithm estimates of hydrologic response were considerably more variable than Wittenberg, reflecting a wider range of parameter uncertainty determined by uniform distributions and the influence of BFI_{max}. While α, β, and k were fitted or derived from measured data (recession limbs), the BFI_{max} parameter is an estimated qualitative value that exerts significant influence ($|\text{tau-b} - b| = 0.75$–$0.84$) in our analysis (Table 4). The range of BFI_{max} uncertainty (0.25–0.80) dictates the wide range of long-term hydrologic response, yielding a BFI ranging from 0.19 to 0.46 for HCW time series (Figure 7). Calculated baseflow differences between algorithms cannot solely be attributed to the sensitivity of the BFI_{max} parameter (Figure 7) as baseflow values produced by $BFI_{max} = 0.8$ (maximum value) did not reach annual estimates of the Wittenberg algorithm. We note that sensitivities of computed baseflows reach a local minimum near $BFI_{max} = 0.5$ where the computed condition number (CN) (Chapra 1997; Lenhart et al. 2002) drops to $CN = +0.65$ to $+0.68$ from maximums that occur near $BFI_{max} = 0.8$ (Figure 7). Differences in the parameterization approach and algorithm structure produce statistically significant differences ($p \leq 0.05$) in hydrologic response in this evaluation. Future studies investigating predictive uncertainty introduced by algorithm structure is therefore warranted.

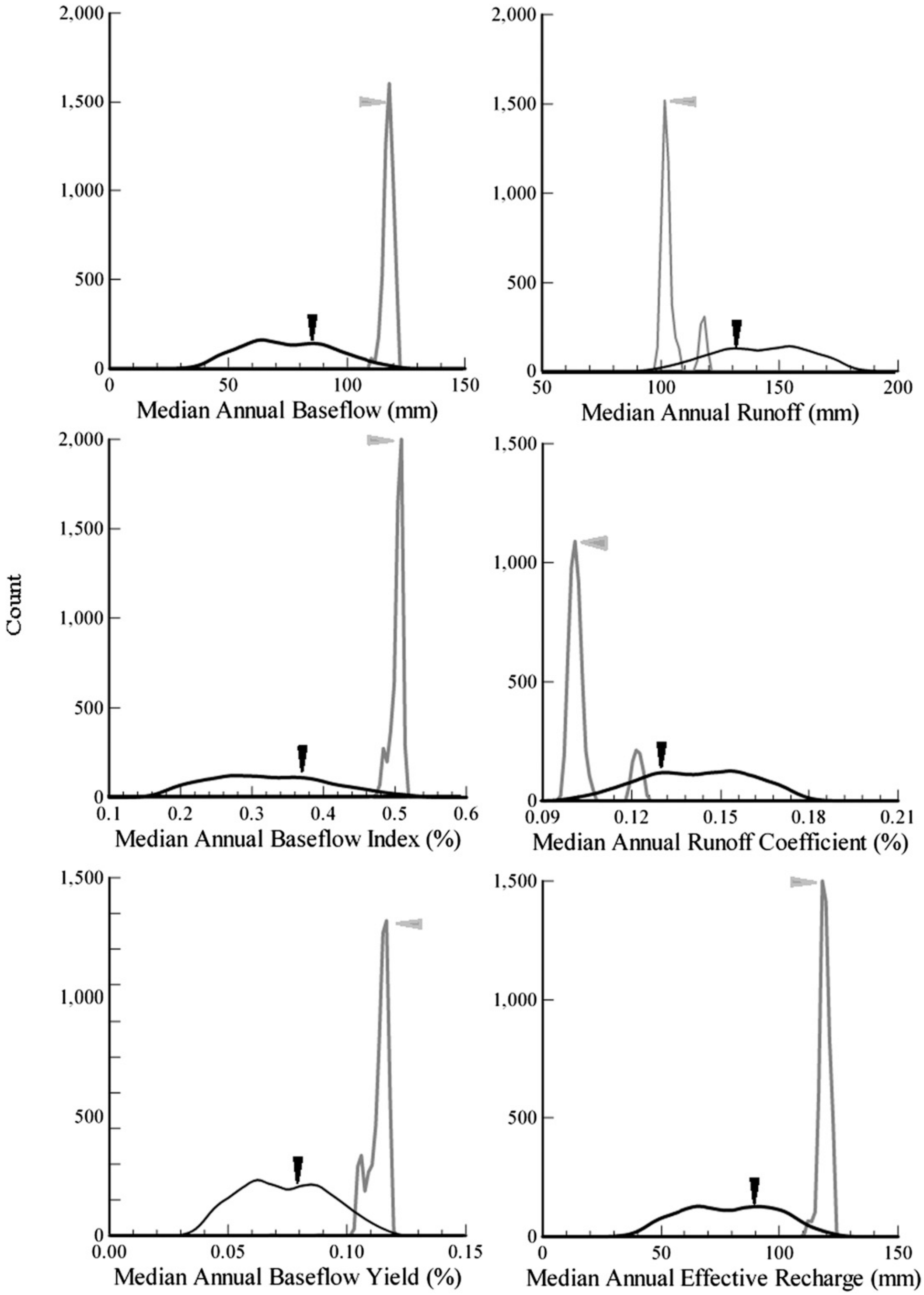

Figure 6. Density functions of median annual (n = 22 years) streamflow metrics calculated from Eckhardt (black) and Wittenberg (gray) separation algorithms for Hinkson Creek (1967–2010; n = 4,000 medians derived from 84 000 annual estimates) located in central Missouri. Arrows demarcate base-case estimates.

Table 4. Sensitivity of annual streamflow metrics expressed as Kendall's tau-b correlation measure calculated from n = 2000 annual medians for the Hinkson Creek watershed, Columbia, Missouri.

	Eckhardt		Wittenberg	
Streamflow metric	BFI_{max}	k	α	β
Baseflow volume (mm)	0.77	−0.22	−0.29	−0.23
Runoff volume (mm)	−0.78	0.22	0.07	−0.05
Effective recharge (mm)	0.84	−0.16	−0.24	−0.22
Runoff coefficient (%)	−0.75	0.25	0.07	−0.06
Baseflow index (%)	0.76	−0.24	−0.06	−0.04
Baseflow yield (%)	0.79	−0.22	−0.06	−0.02

As discussed, automated separation methods are more objective and reproducible than graphical methods. However, the accuracy or precision of those methods as compared against or calibrated to more direct measurements of baseflow (e.g., isotopes, geochemical signatures, etc.) are generally absent for urbanizing watersheds. To advance application and accuracy of separation algorithms, we propose that future evaluations include calibration of model parameters to direct measurements at

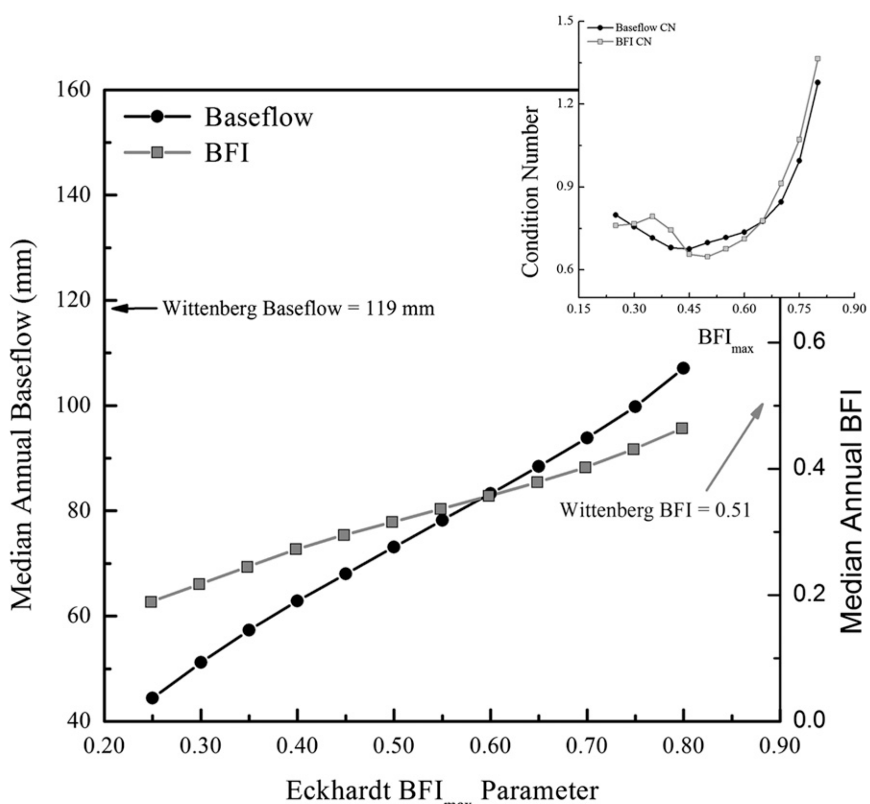

Figure 7. Sensitivity of median annual (n = 22 years) baseflow and baseflow Index to Eckhardt BFI_{max} parameter (1967–2010) for Hinkson Creek, located in central Missouri.

local and regional scales (e.g., Tetzlaff and Soulsby 2008; Gonzales et al. 2009) and relate those calibrated parameters to generally available hydrogeologic data (e.g., Bloomfield et al. 2009).

3.4. Trend analyses

The objective of this investigation included evaluation of sources of uncertainty in annual hydrologic trend analyses using a central U.S. representative watershed: nonlinear precipitation effects, structure of baseflow separation algorithm, and parameter variability. To those ends, we employed two baseflow separation techniques to characterize trends, behavior, and uncertainty of hydrologic response to land use over time predicted by the two algorithms. Case-study results indicate that annual streamflow metrics have not significantly ($p \leq 0.05$) increased or decreased with time from 1967 to 2010 in the HCW as computed by either of two dissimilar baseflow separation algorithms (Table 5 and Figure 8). Several streamflow metrics not adjusted for precipitation influences featured shallow but insignificant ($p > 0.05$) slopes in the direction hypothesized for an urbanizing (less pervious) watershed, including a downward slope for BFI and increases in runoff volume and coefficient. As shown in Figure 5, all HCW streamflow metrics were significantly correlated to precipitation. Therefore, it is not surprising that precipitation adjusted streamflow metric slopes switched direction (four of six metrics) or decreased in magnitude (Table 5 and Figure 8).

Algorithm parameter combinations produced by Monte Carlo simulation did not yield significant time trends for streamflow time series following removal of precipitation influences. The lowest p value (highest significance) achieved for any streamflow metric iteration was $p = 0.07$ (tau-b $= -0.28$) for the adjusted BFI annual time series computed from the Wittenberg algorithm (Figure 9). While the maximum |tau-b| resulted in a p value approaching significance, temporal correlations for the adjusted Wittenberg BFI averaged $p = 0.31$ (|tau-b| ~ 0.16), well less than necessary to reject the null hypothesis. Iterations of the Wittenberg algorithm are predominately either increasing (runoff and runoff coefficient) or decreasing (baseflow and BFI) while adjusted Eckhardt temporal correlations averaged closer to zero (Figure 9). Despite the lack of significant trend resultant from either algorithm, the Wittenberg method that performs best according to π_1 and π_2 measures may serve as a harbinger of hydrologic changes yet to come.

3.5. Implications for the HCW and other urbanizing watersheds

Statistically significant monotonic changes in annual baseflow or runoff metrics were not detected in HCW time series either as base-case estimates or as maximum values that incorporated parameter uncertainties. However, following reduction of time series variance through precipitation adjustment, a parabolic pattern emerged for several streamflow metrics (Figure 8). For example, adjusted baseflows from both algorithms showed declines in volume from the late 1960s through the 1980s, followed by an increase in recent years (2008–10). This pattern also appears in annual runoff volume, runoff coefficient, and effective recharge time series. Despite limited data in recent years ($n = 3$ annual metrics),

Table 5. Monotonic trend analysis statistics for annual streamflow metrics calculated with Eckhardt and Wittenberg algorithms for the Hinkson Creek watershed (1967–2010; n = 22 comparisons) located in Columbia, Missouri. Here, τ is Kendall's tau-b statistic, T is Kendall–Theil slope (metric/year), and p_{yr} is the two-sided p value of time slope.

Streamflow metric	Eckhardt Native units (precipitation adjusted)			Wittenberg Native units (precipitation adjusted)		
	τ	T	P_{yr}	τ	T	P_{yr}
Baseflow volume (mm)	0.14 (−0.07)	1.02 (−0.14)	0.37 (0.69)	0.09 (−0.11)	0.88 (−0.25)	0.57 (0.49)
Runoff volume (mm)	0.13 (0.00)	2.36 (0.03)	0.40 (0.99)	0.18 (0.06)	1.88 (0.20)	0.26 (0.74)
Effective recharge (mm)	0.13 (−0.03)	1.12 (−0.05)	0.43 (0.87)	0.10 (−0.10)	1.00 (−0.34)	0.54 (0.54)
Runoff coefficient (%)	0.13 (−0.07)	0.11 (−0.05)	0.40 (0.67)	0.15 (−0.02)	0.14 (−0.01)	0.34 (0.91)
Baseflow index (%)	−0.10 (−0.04)	−0.05 (−0.02)	0.55 (0.84)	−0.20 (−0.13)	−0.24 (−0.11)	0.21 (0.43)
Baseflow yield (%)	0.12 (−0.07)	0.10 (−0.02)	0.46 (0.67)	0.07 (−0.12)	0.05 (−0.04)	0.69 (0.46)

there is ample anecdotal information to suggest this parabolic pattern may reflect real hydrologic changes.

During the 1970s and 1980s, approximately 54 distributed wastewater treatment facilities (WWTFs) were gradually closed and eventually routed to a regional facility outside the HCW that was constructed in 1983. The estimated cumulative dry weather design flow for the regional facility is approximately 10 million gallons per day (MGD). Effluent from WWTFs represents artificial baseflow (Lerner 2002) and the export of 10 MGD (77 mm annually) may to some extent explain the decline in baseflow volumes from the late 1960s to 1980s (Figure 8). In addition to export of WWTF flows, the establishment of public water supply districts and drinking water wells in the 1960s and 1970s in Boone County (Sturgis 2011) may have influenced regional baseflow patterns.

Increases in computed baseflow for the 2008–10 period from apparent minima in the 1980s could be attributed to exfiltration from expanded drinking water, stormwater, and wastewater conveyance networks necessary to serve the growing Columbia and Boone County populations (Figure 2). Lerner (Lerner 2002) suggested that up to 300 mm yr^{-1} of recharge can be attributed to subsurface infrastructure. We contend that parabolic (nonmonotonic) patterns in baseflow could be the result of gradual effluent loss followed by an increase in conveyance exfiltration. Isotope signatures, solute balances, and numerical modeling are presented by Lerner (Lerner 2002) and Sidle and Lee (Sidle and Lee 1999) as methods to quantify infrastructure contributions to baseflow and recharge.

Detention, seepage, and timed maintenance releases from urban lakes and ponds are potential but contextually unquantified processes in HCW time series. Removal and/or construction of wetlands, ponds, or lakes could alter historic runoff and thus baseflow regimes (LeBlanc et al. 1997; Kochendorfer and Hubbart 2010). Similar to impervious surfaces, detention and retention facilities and other urban ponds

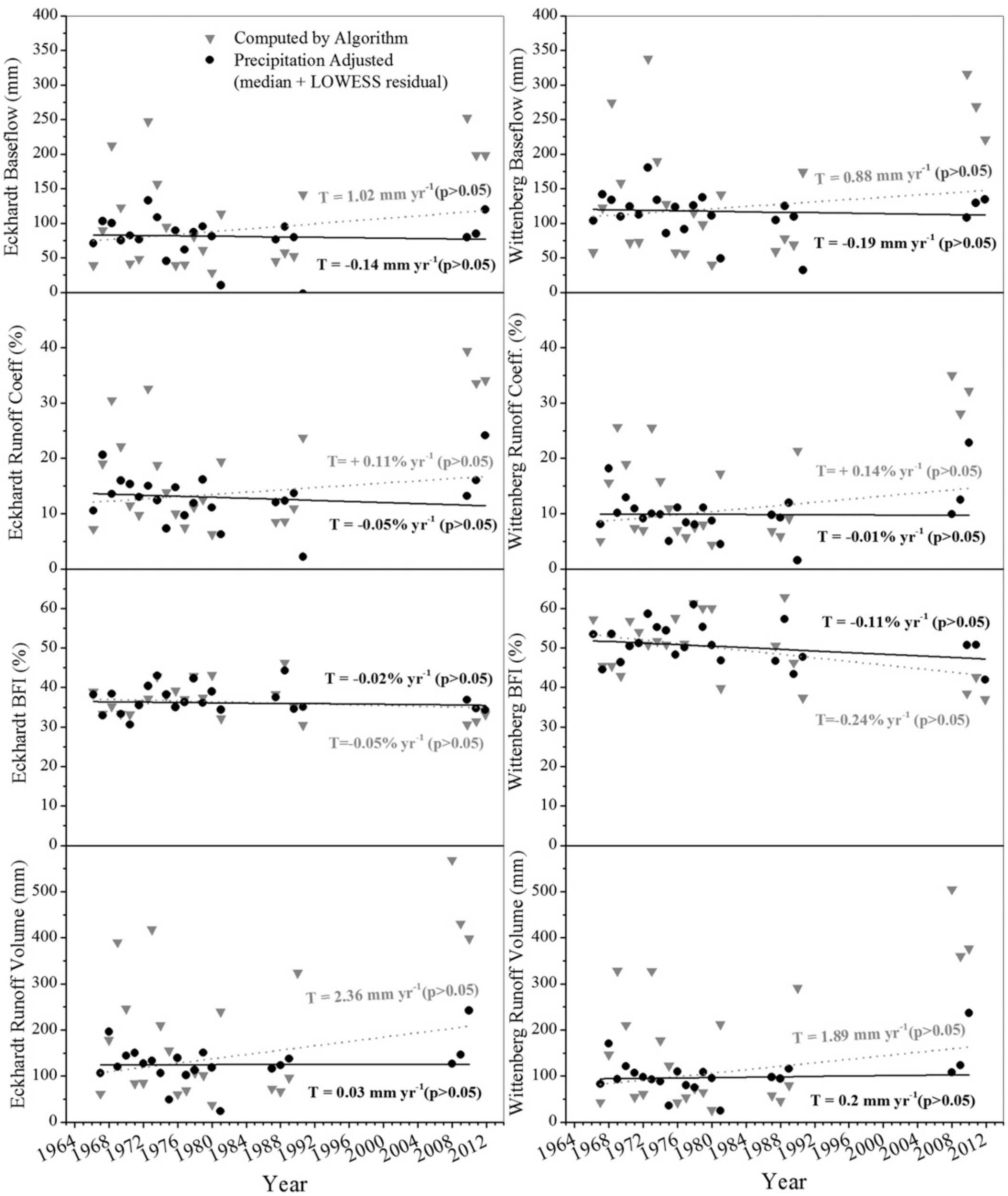

Figure 8. Base-case monotonic time trends for native and adjusted annual streamflow metric time series for Hinkson Creek (1967–2010) located in central Missouri. Note baseflow yield and effective recharge are not shown.

have replaced roots, leaf litter, and forest canopies that once dominated many urban landscapes (Hubbart et al. 2011). Further, urban lakes exhibit many differences from other lakes (Birch and McCaskie 1999) in that they are shallower and tend to be hypertrophic. Knowledge of urban lakes management effects on baseflows and

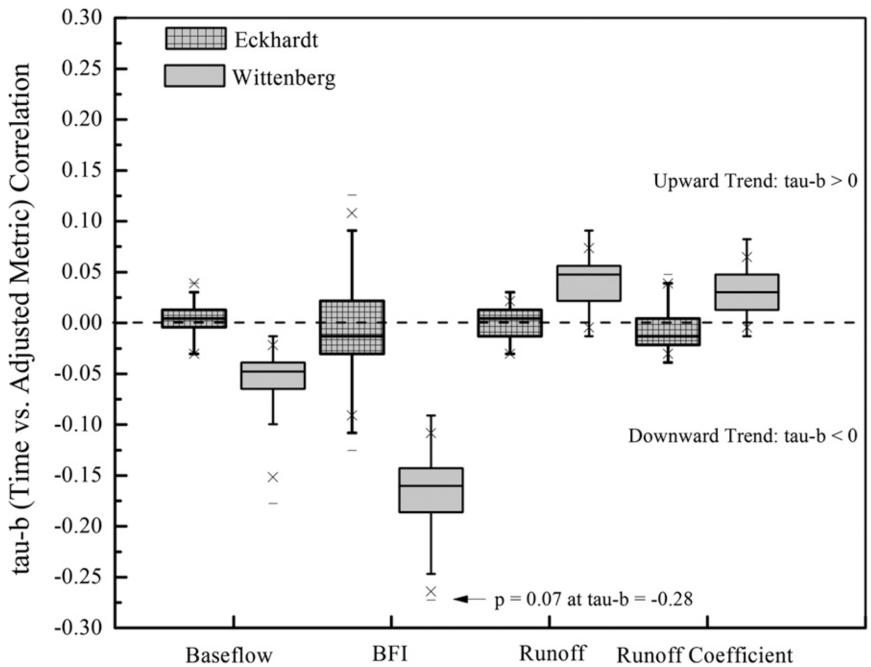

Figure 9. Precipitation adjusted annual time trends for each of *n* = 2000 Monte Carlo simulations for Hinkson Creek located in central Missouri. Note the baseflow yield and effective recharge are not shown.

urban aquatic ecosystem health remains poor. Future studies should therefore seek to investigate the effects of lakes to better assess the water balance, baseflow regime (Lerner 2002), and health of aquatic ecosystem health in urban areas (Birch and McCaskie 1999).

These pathways and algorithm differences underscore the complexities of identifying quantitatively hydrologic changes and specifying volume reductions in urbanizing watersheds. The Ecological Limits of Hydrologic Alteration (ELOHA) framework proposed by Poff et al. (Poff et al. 2010) is an iterative and adaptive process whereby changes in hydrologic response are related to changes in aquatic biota (i.e., TMDL and stressor–response analysis). An initial component of ELOHA framework requires quantifying hydrologic alteration compared to baseline (predevelopment) conditions. The trend analysis presented in this paper did not detect statistically significant changes in evaluated streamflow metrics over the available period of record (1966–2010) in the HCW. These results should be interpreted cautiously in the context of the ELOHA framework for several reasons including the following: 1) the first year of gauged streamflows (1966) does not reflect a predevelopment (historical) condition, 2) ecology-based metrics such as those considered by Henriksen et al. (Henriksen et al. 2006) or Richter et al. (Richter et al. 1996) were not included in the trend analysis, and 3) streamflows evaluated at annual time steps may not capture seasonal hydrograph changes that are critical to life cycle needs (i.e., reproduction periods etc.). However, as described by Booth et al. (Booth et al. 2002) and Brown (Brown 2010), a natural flow regime may not be achievable in some developed watersheds. Therefore, time series start dates, such as in the HCW (1966), may be required to represent a suitable or best-available baseline.

4. Conclusions

We evaluated three sources of uncertainty in annual hydrologic trend analyses: nonlinear precipitation effects, structure of baseflow separation algorithm, and parameter variability. Precipitation accounted for greater than 50% of the variation in five of six hydrologic response metrics. The relationship between streamflow metrics (except BFI) and annual precipitation featured a change point at 900–1000 mm where streamflow per unit precipitation increased. Hydrologic response metrics produced by two baseflow separation algorithms having dissimilar assumptions and structures produced statistically different ($p \leq 0.05$) estimates (29% difference) and distributions of streamflow metrics. The nonlinear storage algorithm developed by Wittenberg produced more precise estimates of streamflow metrics than the Eckhardt model based on Monte Carlo simulation of parameter uncertainty. While neither algorithm yielded a statistically significant ($p \leq 0.05$) monotonic temporal trend, the best-performing Wittenberg model achieved comparatively greater p values (stronger relative trend) in directions expected for an urbanizing watershed (i.e., lower baseflows and greater runoff). For these reasons, we conclude the Wittenberg algorithm provides a more reliable estimate of hydrologic response in our representative urban watershed.

In the absence of direct tracer measurements (a common and broadly applicable data gap) to serve as calibration targets, we conclude that uncertainties associated with precipitation relationships, algorithm structure, and parameter uncertainty should be included in trend analyses seeking to evaluate deviations from baseline or reference hydrologic conditions (i.e., streamflow alteration). This article provides a methodology other investigators could follow wishing to evaluate streamflow alteration in urban watersheds and therefore advances the capacity for science-based policies. Further, hydrologic pathways (i.e., urban recharge and WWTP flows) characteristic of urbanizing environments may confound or challenge investigators seeking to quantify temporal changes. We note that baseflow separation algorithms do not intrinsically describe the source of baseflow or runoff. We therefore contend that detecting hydrologic alteration in urbanizing watersheds may require more comprehensive considerations of urban hydrologic processes and techniques including use of stable isotope methodologies.

Acknowledgments. Support provided by the University of Missouri School of Natural Resources and the Interdisciplinary Hydrology Laboratory. The authors are grateful for comments provided by multiple reviewers whose insights improved the quality of the article.

References

Anderson, J., E. Hardy, J. Roach, and R. Witmer, 1976: A land use and land cover classification system for use with remote sensor data. Geological Survey Professional Paper 964, 41 pp.

Arnold, J., and P. Allen, 1999: Automated methods for estimating baseflow and ground water recharge from streamflow records. *J. Amer. Water Resour. Assoc.,* **35,** 411–424.

Barnes, B., 1939: The structure of discharge-recession curves. *Trans. Amer. Geophys. Union,* **20,** 721–725.

Bates, D., and D. Watts, 1988: *Nonlinear Regression Analysis and Its Applications.* Wiley, 359 pp.

Bernhardt, E. S., and M. A. Palmer, 2007: Restoring streams in an urbanizing world. *Freshwater Biol.,* **52,** 738–751.

Beven, K., 1993: Prophecy, reality and uncertainty in distributed hydrological modeling. *Adv. Water Resour.,* **16,** 41–51.

——, and J. Freer, 2001: Equifinality, data assimilation, and uncertainty estimation in mechanistic modeling of complex environmental systems using the GLUE methodology. *J. Hydrol.,* **249,** 11–29.

Birch, S., and J. McCaskie, 1999: Shallow urban lakes: A challenge for lake management. *Hydrobiologia,* **395–396,** 365–377.

Birtles, A., 1978: Identification and separation of major baseflow components from a stream hydrograph. *Water Resour. Res.,* **14,** 791–803.

Bloomfield, J. P., D. J. Allen, and K. J. Griffiths, 2009: Examining geological controls on baseflow index (BFI) using regression analysis: An illustration from the Thames basin, UK. *J. Hydrol.,* **373,** 164–176.

Booth, D., D. Hartley, and R. Jackson, 2002: Forest cover, impervious surface area, and the mitigation of stormwater impacts. *J. Amer. Water Resour. Assoc.,* **38,** 835–845.

Brandes, D., G. Cavallo, and M. Nilson, 2005: Baseflow trends in urbanizing watersheds of the Delaware River basin. *J. Amer. Water Resour. Assoc.,* **41,** 1377–1391.

Brown, T., 2010: Can volume-based stormwater criteria make a difference to receiving stream health? *Water Res. Impact,* **12,** 5–8.

Brutsaert, W., and J. Nieber, 1977: Regionalized drought flow hydrographs from a mature glaciated plateau. *Water Resour. Res.,* **13,** 637–643.

Chapman, S. S., J. M. Omernik, G. E. Griffith, W. A. Schroeder, T. A. Nigh, and T. F. Wilton, 2002: Ecoregions of Iowa and Missouri (map scale 1:1,800,000). U.S. Geological Survey Poster, 1 pp.

Chapman, T., 1999: A comparison of algorithms for streamflow recession and baseflow separation. *Hydrol. Processes,* **13,** 701–714.

Chapra, S., 1997: *Surface Water Quality Modeling.* McGraw-Hill, 844 pp.

Cleveland, W., and S. Devlin, 1988: Locally-weighted regression: An approach to regression analysis by local fitting. *J. Amer. Stat. Assoc.,* **83,** 596–610.

Conover, W., 1980: *Practical Non-Parametric Statistics.* 2nd ed. John Wiley and Sons, 493 pp.

Coutagne, A., 1948: Les variations de debit en periode non infuencee par les precipitations. *Houille Blanche,* **3,** 416–436.

Eckhardt, K., 2005: How to construct recursive digital filters for baseflow separation. *Hydrol. Processes,* **19,** 507–515.

——, 2008: A comparison of baseflow indices, which were calculated with seven different baseflow separation methods. *J. Hydrol.,* **352,** 168–173.

Ellins, K., A. Roman-Mas, and R. Lee, 1990: Using 222Rn to examine groundwater/surface discharge interaction in the Rio Grande de Manati, Puerto Rico. *J. Hydrol.,* **115,** 319–341.

Esralew, R., and J. Lewis, 2010: Trends in baseflow, total flow, and base-flow index of selected streams in Oklahoma through 2008. U.S. Geological Survey Scientific Investigations Rep. 2010-5104., 143 pp.

Furey, P., and V. Gupta, 2001: A physically based filter for separating baseflow from streamflow time series. *Water Resour. Res.,* **37,** 2709–2722.

Genereux, D., and R. Hooper, 1998: Oxygen and hydrogen isotopes in rainfall-runoff studies. *Isotope Tracers in Catchment Hydrology,* C. Kendall and J. McDonnell, Eds., Elsevier, 319–343.

Gonzales, A., J. Nonner, J. Heijkers, and S. Uhlenbrook, 2009: Comparison of different base flow separation methods in a lowland catchment. *Hydrol. Earth Syst. Sci.,* **13,** 2055–2068.

Goodrich, D., L. Lane, R. Shillito, S. Miller, K. Syed, and D. Woolhiser, 1997: Linearity of basin response as a function of scale in a semiarid watershed. *Water Resour. Res.,* **33,** 2951–2965.

Harlan, J., 1997: Land use/land cover prepared from U.S. Geological Survey notes. Missouri Spatial Data Information Service Dataset.

Helsel, D., and R. Hirsch, 2002: *Statistical Methods in Water Resources.* Elsevier, 522 pp.

Henriksen, J., J. Heasley, J. G. Kennen, and S. Nieswand, 2006: User's manual for the Hydroecological Integrity Assessment Process software (including the New Jersey assessment tools). U.S. Geological Survey Rep. 2006-1093, 80 pp.

Hirsch, R., R. Alexander, and R. Smith, 1991: Selection of methods for the detection and estimation of trends in water quality. *Water Resour. Res.,* **27,** 803–813.

Hubbart, J. A., R.-M. Muzika, D. Huang, and A. Robinson, 2011: Bottomland Hardwood forest influence on soil water consumption in an urban floodplain: Potential to improve flood storage capacity and reduce stormwater runoff. *Watershed Science Bulletin,* No. 3, Association of Watershed and Stormwater Professionals, Elliot City, MD, 34–43.

Jones, J., T. Earles, E. Fassman, E. Herricks, B. Urbonas, and M. Clary, 2005: Urban storm-water regulations—Are impervious area limits a good idea? *J. Environ. Eng.,* **131,** 176–179.

Kish, G., C. Stringer, M. Stewart, M. Rains, and A. Torres, 2010: A geochemical mass-balance method for base-flow separation, upper Hillsborough River watershed, west-central Florida, 2003-2005 and 2009. U.S. Geological Survey Scientific Investigations Rep. 2010-5092, 32 pp.

Kochendorfer, J., and J. A. Hubbart, 2010: The roles of precipitation increases and rural land-use changes in streamflow trends in the upper Mississippi River. *Earth Interact.,* **14,** doi:10.1175/2010EI316.1.

Kokkonen, T., H. Koivusalo, T. Karvonen, B. Coke, and A. Jakeman, 2004: Exploring streamflow response to effective rainfall across event magnitude scale. *Hydrol. Processes,* **18,** 1467–1486.

Kusumastuti, D., I. Struthers, M. Sivapalan, and D. Reynolds, 2007: Threshold effects in catchment storm response and the occurrence and magnitude of flood events: Implications for flood frequency. *Hydrol. Earth Syst. Sci.,* **1,** 1515–1528.

LeBlanc, R. T., R. D. Brown, and J. E. FitzGibbon, 1997: Modeling the effects of land use change on the water temperature in unregulated urban streams. *J. Environ. Manage.,* **49,** 445–469.

Lenhart, T., K. Eckhardt, N. Fohrer, and H. Frede, 2002: Comparison of two different approaches of sensitivity analysis. *Phys. Chem. Earth,* **27,** 645–654.

Lerch, R., C. Wicks, and P. Moss, 2005: Hydrologic characterization of two karst recharge areas in Boone County, Missouri. *J. Caves Karst Stud.,* **67,** 158–173.

Lerner, D., 2002: Identifying and quantifying urban recharge: a review. *Hydrogeol. J.,* **10,** 143–152.

Maillet, E., 1905: *Essais d'Hydraulique Souterraine et Fluviale.* Hermann, 218 pp.

MDEP, 2006: Barberry Creek total maximum daily load (TMDL). Maine Department of Environmental Protection Rep. DEPLW0172, 41 pp.

McDonnell, J. J., and Coauthors, 2007: Moving beyond heterogeneity and process complexity: A new vision for watershed hydrology. *Water Resour. Res.,* **43,** 1–6.

McGrath, G., C. Hinz, and M. Sivapalan, 2007: Temporal dynamics of hydrological threshold events. *Hydrol. Earth Syst. Sci.,* **11,** 923–938.

Meyer, S., 2005: Analysis of baseflow trends in urban streams, northeastern Illinois, USA. *Hydrogeol. J.,* **13,** 871–885.

Miller, D., and J. Vandike, 1997: Groundwater resources of Missouri. Missouri Department of Natural Resources Division of Geology and Land Survey Water Resources Rep. 46., 136 pp.

Moore, R., 1997: Storage–outflow modeling of streamflow recessions with application to shallow-soil forested catchment. *J. Hydrol.,* **198,** 260–270.

Morgan, M., and M. Henrion, 2003: *Uncertainty: A Guide to Dealing with Uncertainty in Quantitative Risk and Policy Analyses.* Cambridge University Press, 325 pp.

Mostaghimi, S., K. Brannan, T. Dillaha, and A. Bruggeman, 2001: Best management practices for nonpoint source pollution control: Selection and assessment. *Agricultural Nonpoint Source Pollution: Watershed Management and Hydrology,* A. Shirmohammadi and W. Ritter, Eds., CRC Press, 352 pp.

MRCC, 2010: Annual data download for cooperative stations 231790 (Columbia Muni AP) and 231791 (Columbia Rgnl AP). Midwest Regional Climatic Center Database.

Nathan, R., and T. McMahon, 1990: Evaluation of automated techniques for baseflow and recession analyses. *Water Resour. Res.,* **26,** 1465–1473.

Newbury, R., J. Cherry, and R. Cox, 1969: Groundwater-streamflow systems in Wilson Creek Experimental Watershed, Manitoba. *Can. J. Earth Sci.,* **6,** 613–623.

NRC, 2008: *Urban Stormwater Management in the United States.* National Academies Press, 529 pp.

O'Driscoll, M., S. Clinton, A. Jefferson, A. Manda, and S. McMillan, 2010: Urbanization effects on watershed hydrology and in-stream processes in the southern United States. *Water,* **2,** 605–648.

Padilla, A., A. Pulido-Bosch, and A. Mangin, 1994: Relative importance of baseflow and quickflow from hydrographs of karst spring. *Ground Water,* **32,** 267–277.

Paul, M., and J. Meyer, 2001: Streams in the urban landscape. *Annu. Rev. Ecol. Syst.,* **32,** 333–365.

Pazwash, H., 2011: *Urban Storm Water Management.* CRC Press, 534 pp.

Pelletier, G., 2009: YASAIw.xla—A modified version of an open source add-in for Excel to provide additional functions for Monte Carlo simulation. Washington Department of Ecology Rep., 17 pp.

Peters, E., and H. van Lanen, 2005: Separation of baseflow from streamflow using groundwater levels—Illustrated for the Pang catchment (UK). *Hydrol. Processes,* **19,** 921–936.

Poff, N., and Coauthors, 2010: The ecological limits of hydrologic alternation (ELOHA): A new framework for developing regional environmental flow standards. *Freshwater Biol.,* **55,** 147–170.

Richter, B., J. Baumgartner, J. Powell, and D. Braun, 1996: A method for assessing hydrologic alteration within ecosystems. *Conserv. Biol.,* **10,** 1163–1174.

Rose, S., and N. Peters, 2001: Effects of urbanization on streamflow in the Atlanta area (Georgia, USA): A comparative hydrological approach. *Hydrol. Processes,* **15,** 1441–1457.

Rutledge, A., 1998: Computer programs for describing the recession of ground-water discharge and for estimating mean ground-water recharge and discharge from streamflow records update. U.S. Geological Survey Water-Resources Investigation Rep. 1998-4148, 52 pp.

Sharp, J., 1984: Hydrogeologic characteristics of shallow glacial drift aquifers in dissected till plains (north-central Missouri). *Ground Water,* **22,** 683–689.

Sidle, W., and P. Lee, 1999: Urban stormwater tracing with the naturally occurring deuterium isotope. *Water Environ. Res.,* **71,** 1251–1256.

Smith, R., and R. Hebbert, 1979: A Monte Carlo analysis of the hydrologic effects of spatial variability of infiltration. *Water Resour. Res.,* **15,** 419–429.

Sophocleus, M., 2002: Interactions between groundwater and surface water: The state of the science. *Hydrogeol. J.,* **10,** 52–67.

Spinello, A., and D. Simmons, 1992: Baseflow of 10 south-shore streams, Long Island, New York, 1976–1985, and the effects of urbanization on baseflow and flow duration. U.S. Geological Survey Water-Resources Investigations Rep. 90-4205, 34 pp.

Starbuck, E., 2007: Uppermost bedrock geology and major alluvial deposits located within the state of Missouri. Geospatial dataset compiled by Missouri Department of Natural Resource Division of Geology and Land Survey, Rolla, Missouri.

Sturgis, S., 2011: Census of Missouri public water systems. Missouri Department of Natural Resources, Public Drinking Water Branch. Jefferson City, Missouri.

Sujono, J., S. Shikasho, and D. Hiramatsu, 2004: A comparison of techniques for hydrograph recession analysis. *Hydrol. Processes,* **18,** 403–413.

Tallaksen, L. M., 1995: A review of baseflow recession analysis. *J. Hydrol.,* **165,** 349–370.

Tetzlaff, D., and C. Soulsby, 2008: Sources of baseflow in larger catchments – Using tracers to develop a holistic understanding of runoff generation. *J. Hydrol.,* **359,** 287–302.

Thom, R. H., and J. H. Wilson, 1980: The natural division of Missouri. *Trans. Mo. Acad. Sci.,* **14,** 1–23.

Unklesbay, A., 1952: *Geology of Boone County, Missouri.* 2nd series, Vol. 33, Missouri Geology and Land Survey and Water Resources, 159 pp.

U.S. EPA, 2011: Total maximum daily load for Hinkson Creek (MO_IOO7 aDd _1008). U.S. Environmental Protection Agency Rep., 88 pp.

USGS, 1996: Geo-dataset delineating the state quaternary geology of Missouri based on Anderson, K.H. and others, 1979, Geologic Map of Missouri. Missouri Department of Natural Resources Division of Geology and Land Survey Database.

Vogel, R., and C. Kroll, 1996: Estimation of baseflow recession constants. *Water Resour. Manage.,* **10,** 303–320.

VTDEC, 2006: Potash Brook total maximum daily load study. Vermont Department of Environmental Conservation Rep., 31 pp.

——, 2009: Total maximum daily loads for Moon, Stevens and Rugg Brooks. Vermont Department of Environmental Conservation Rep., 39 pp.

Walsh, C., A. Roy, J. Feminella, P. Cottingham, P. Groffman, and R. Morgan, 2005: The urban stream syndrome: Current knowledge and the search for a cure. *J. N. Amer. Benthol. Soc.,* **24,** 706–723.

Wels, C., R. Cornet, and B. Lazerte, 1991: Hydrograph separation: A comparison of geochemical and isotopic tracers. *J. Hydrol.,* **122,** 253–274.

Wenger, S., and Coauthors, 2009: Twenty-six key research questions in urban stream ecology: an assessment of the state of the science. *J. N. Amer. Benthol. Soc.,* **28,** 1080–1098.

Wicks, C., 1997: Origins of groundwater in a fluviokarst basin: Bonne Femme basin in central Missouri, USA. *Hydrogeol. J.,* **5,** 89–96.

Wittenberg, H., 1999: Baseflow recession and recharge as nonlinear storage processes. *Hydrol. Processes,* **13,** 715–726.

——, 2003: Effects of season and man-made changes on baseflow and flow recession: Case studies. *Hydrol. Processes,* **17,** 2113–2123.

Young, F., C. Radatz, and C. Marshall, 2001: Soil survey of Boone County, Missouri. U.S. Department of Agriculture Natural Resources Conservation Service Rep., 318 pp.